

JYX



This is a self-archived version of an original article. This version may differ from the original in pagination and typographic details.

Author(s): ALICE Collaboration

Title: Elliptic Flow of Electrons from Beauty-Hadron Decays in Pb-Pb Collisions at $\sqrt{s_{NN}} = 5.02$ TeV

Year: 2021

Version: Published version

Copyright: © 2021 CERN, for the ALICE Collaboration

Rights: CC BY 4.0

Rights url: <https://creativecommons.org/licenses/by/4.0/>


Please cite the original version:

ALICE Collaboration. (2021). Elliptic Flow of Electrons from Beauty-Hadron Decays in Pb-Pb Collisions at $\sqrt{s_{NN}} = 5.02$ TeV. *Physical Review Letters*, 126(16), Article 162001.

<https://doi.org/10.1103/PhysRevLett.126.162001>

Elliptic Flow of Electrons from Beauty-Hadron Decays in Pb-Pb Collisions at $\sqrt{s_{NN}} = 5.02$ TeV

S. Acharya *et al.**
(ALICE Collaboration)

 (Received 23 June 2020; revised 27 January 2021; accepted 9 March 2021; published 19 April 2021)

The elliptic flow of electrons from beauty hadron decays at midrapidity ($|y| < 0.8$) is measured in Pb-Pb collisions at $\sqrt{s_{NN}} = 5.02$ TeV with the ALICE detector at the LHC. The azimuthal distribution of the particles produced in the collisions can be parametrized with a Fourier expansion, in which the second harmonic coefficient represents the elliptic flow, v_2 . The v_2 coefficient of electrons from beauty hadron decays is measured for the first time in the transverse momentum (p_T) range 1.3–6 GeV/ c in the centrality class 30%–50%. The measurement of electrons from beauty-hadron decays exploits their larger mean proper decay length $c\tau \approx 500$ μm compared to that of charm hadrons and most of the other background sources. The v_2 of electrons from beauty hadron decays at midrapidity is found to be positive with a significance of 3.75σ . The results provide insights into the degree of thermalization of beauty quarks in the medium. A model assuming full thermalization of beauty quarks is strongly disfavored by the measurement at high p_T , but is in agreement with the results at low p_T . Transport models including substantial interactions of beauty quarks with an expanding strongly interacting medium describe the measurement within uncertainties.

DOI: [10.1103/PhysRevLett.126.162001](https://doi.org/10.1103/PhysRevLett.126.162001)

The main goal of the ALICE experiment [1] is the study of strongly interacting matter at the high energy density and temperature reached in ultrarelativistic heavy-ion collisions at the Large Hadron Collider (LHC). In these collisions, the formation of a deconfined state of quarks and gluons, the quark-gluon plasma (QGP), is predicted by quantum chromodynamic (QCD) calculations on the lattice [2–6]. Because of their large masses, heavy quarks [charm (c) and beauty (b)] are mainly produced in hard scattering processes at the initial stage of the collision, before the formation of the QGP. Subsequently, they interact with the QGP, losing energy via radiative [7,8] and collisional scattering [9–11] processes. Heavy-flavor hadrons and their decay products are thus effective probes to study the properties of the medium created in heavy-ion collisions. In non-central collisions, interactions among the medium constituents translate the initial spatial anisotropy in the coordinate space of nucleons participating in the collision into a momentum space anisotropy of produced particles in the final state [12]. The momentum anisotropies are characterized by the flow harmonic coefficients v_n from the Fourier expansion of the particle azimuthal distribution with respect to the azimuthal

angle of the symmetry plane for the n th harmonic. The dominant flow harmonic is the elliptic flow v_2 [13]. At low transverse momentum, $p_T < 3$ GeV/ c , the measurements of positive v_2 are considered a manifestation of the collective hydrodynamical expansion of the medium [14–17]. At high p_T ($p_T > 3$ GeV/ c), v_2 measurements give insight into the path-length dependence of the in-medium parton energy loss [18–20].

The measurements of D meson and J/ψ v_2 in heavy-ion collisions, performed at RHIC in Au-Au collisions at $\sqrt{s_{NN}} = 200$ GeV [21] and at the LHC in Pb-Pb collisions at $\sqrt{s_{NN}} = 2.76$ and 5.02 TeV [22–28], suggest that the interaction of charm quarks with the medium is sufficiently strong to make them thermalize and thereby take part in the collective flow of the medium [29–35]. Additional mechanisms, like coalescence of charm quarks with the lighter quarks produced in the medium, can contribute to the flow of heavy-flavor particles [36]. Models consistent with the flow measurements of charm quarks have charm quark thermalization times of the order of the system lifetime (≈ 10 fm/ c) [29]. This indicates that low- p_T charm quarks may be fully thermalized in the QGP due to their interactions with the medium. A nonthermalized probe is required to assess the interaction with the medium more thoroughly, with the heavier beauty quarks being a natural candidate. It has been predicted by transport models that beauty quarks may experience sufficient scattering in the medium to produce positive v_2 values [34,37,38].

Measurements of the anisotropic flow of leptons from combined charm and beauty hadron decays also showed

*Full author list given at the end of the article.

Published by the American Physical Society under the terms of the [Creative Commons Attribution 4.0 International license](https://creativecommons.org/licenses/by/4.0/). Further distribution of this work must maintain attribution to the author(s) and the published article's title, journal citation, and DOI.

that heavy quarks undergo significant rescattering in the medium and thus participate in its expansion [39–42]. However, strong conclusions about the dynamics of the beauty quark alone cannot be drawn from those measurements, and separation of the charm and beauty contribution is necessary. Some anisotropic flow measurements of open-beauty do exist. The measured v_2 coefficient of the non-prompt J/ψ , which is dominated by $B \rightarrow J/\psi$ carried out by the CMS Collaboration is consistent with zero within large experimental uncertainties for $p_T > 3$ GeV/ c [43]. Recent measurements of the v_2 coefficient for $\Upsilon(1S)$ by ALICE [44], for $p_T < 15$ GeV/ c , are consistent both with zero and with the small value predicted by transport models [45,46] within uncertainties. Studies based on the Blast-Wave model show that, due to the large $\Upsilon(1S)$ mass, even with full thermalization a sizable elliptic flow would only be expected at $p_T > 10$ GeV/ c [47]. Hence lighter beauty hadrons, and their decay particles, would provide important additional information for the study of the interaction of beauty quarks with the medium. Recent ATLAS measurement of v_2 of muons from heavy-flavor hadron decays, including the separation of charm and beauty quark contributions, in Pb-Pb collisions at $\sqrt{s_{NN}} = 5.02$ TeV for $p_T > 4$ GeV/ c revealed smaller flow coefficients for muons from beauty hadron decays compared to those from charm hadrons [48].

In this Letter, the measurement of the v_2 of electrons (and positrons) from beauty hadron decays at midrapidity ($|y| < 0.8$) in Pb-Pb collisions at $\sqrt{s_{NN}} = 5.02$ TeV recorded in 2018 with the ALICE detector is reported. The measurement is performed for the first time in the p_T interval $1.3 < p_T < 6$ GeV/ c . The measurement is based on 77×10^6 minimum bias Pb-Pb collisions with a primary vertex reconstructed within ± 10 cm from the detector center [49] in the 30%–50% centrality interval. Two forward and backward scintillator arrays (V0A and V0C) are used to determine the collision centrality [50,51].

Electron candidate tracks, reconstructed with up to 159 measurement points in the Time Projection Chamber (TPC) and up to 6 in the Inner Tracking System (ITS), are required to fulfill standard track selection criteria as listed in Refs. [22,52]. To minimize the contribution of electrons from photon conversions in the detector material of the ITS and the fraction of tracks with misassociated hits, tracks are required to have associated hits in both Silicon-Pixel-Detector (SPD) layers, which constitute the two innermost layers of the ITS. This requirement removes most electrons from photon conversion produced outside the first SPD layer from the track sample. However, in the high-multiplicity environment of heavy-ion collisions, some of these can be misassociated with hits in the SPD layers produced by other particles. Electron identification is done using the TPC and the Time Of Flight detector (TOF) [22,52]. Electrons are identified by requiring the measured time-of-flight up to the TOF radius of 3.8 m on average to be

within 3σ of the expected value for electrons and their specific energy loss dE/dx in the TPC to be within -1σ and $+3\sigma$ with respect to the expected dE/dx of electrons.

Electrons passing the track and identification selection criteria originate, besides from beauty-hadron decays, from Dalitz and dielectron decays of prompt light neutral mesons and charmonium states, photon conversions in the detector material, semileptonic decays of prompt-charm hadrons and decay chains of hadrons carrying a strange (or anti-strange) quark. Measurements of electrons from beauty-hadron decays exploit their larger average impact parameter (d_0), defined as distance of closest approach to the primary vertex in the plane transverse to the beam line, compared to that of charm hadrons and most other background sources. The sign of the impact parameter value is determined from the relative position of the track to the primary vertex, i.e., if the primary vertex is on the left- or right-hand side of the track with respect to the particle momentum direction in the transverse plane. The impact parameter is multiplied with the sign of the particle charge and the magnetic field configuration [52]. Electrons from photon conversions in the detector material are created at some distance from the primary vertex and in the direction of the photon. Their tracks bend away from the primary vertex, leading to an asymmetry with a mean impact parameter $d_0 < 0$. This asymmetric impact parameter distribution allows for a better separation from the other electron sources, which are mostly symmetric around 0.

The momentum anisotropies are characterized by the flow harmonic coefficients v_n and azimuthal angle of the symmetry plane of the n th harmonic Ψ_n from the Fourier expansion of particle azimuthal distribution in the plane transverse to the beam direction [53]. The experimental estimate of the symmetry plane for the 2nd harmonic of the collision geometry in the azimuthal direction, the event plane Ψ_2 , is determined using the signals produced by charged particles in the eight azimuthal sectors of each V0 array. Nonuniformities in the V0 acceptance and efficiency are corrected for using the procedure described in Ref. [54].

The $v_2\{\text{EP}\}$ is given by

$$v_2\{\text{EP}\} = \frac{1}{R_2} \frac{\pi}{4} \frac{N_{\text{in}} - N_{\text{out}}}{N_{\text{in}} + N_{\text{out}}}, \quad (1)$$

where N_{in} and N_{out} are the number of beauty-decay electrons in two 90° -wide intervals of $\Delta\varphi = \varphi - \Psi_2$: in plane ($-\pi/4 < \Delta\varphi < \pi/4$ and $3\pi/4 < \Delta\varphi < 5\pi/4$) and out of plane ($\pi/4 < \Delta\varphi < 3\pi/4$ and $5\pi/4 < \Delta\varphi < 7\pi/4$), respectively. The resolution (R_2) of the event plane is measured with the three subevents method [25]. The subevents are defined according to the signals in the V0 detectors (both A and C sides) and the tracks in positive ($0 < \eta < 0.8$) and negative ($-0.8 < \eta < 0$) pseudorapidity regions of the TPC. R_2 is calculated in 1% centrality intervals and a weighted average for the 30%–50% interval

is obtained using the number of binary nucleon-nucleon collisions as weights [25]. The average R_2 value in the 30%–50% centrality class is 0.77 [24].

The N_{in} and N_{out} yields of electrons from beauty-hadron decays are extracted by fitting the impact parameter distribution of all electron candidates in data with Monte Carlo (MC) templates for different electron sources [52]. A MC sample of minimum-bias (MB) Pb-Pb collisions at $\sqrt{s_{NN}} = 5.02$ TeV, generated with HIJING v1.36 [55], is used to obtain the impact parameter distributions of photon conversions and Dalitz decays. To increase the sample of electrons from charm- and beauty-hadron decays, a sample of charm and beauty quarks generated with PYTHIA6 [56] is embedded into each Hijing MC event. The generated particles are propagated through the ALICE apparatus using GEANT3 [57]. Four classes of electron sources are used: electrons from beauty-hadron decays, from charm-hadron decays, from photon conversions, and from all other processes, the latter being dominated by Dalitz decays of light neutral mesons. The Dalitz decays of light neutral mesons happen essentially at the interaction vertex as does the production of most of the remaining hadron contamination. Thus, the impact parameter distributions of the reconstructed tracks are very similar and represent the p_T -dependent impact parameter resolution. The uncertainty due to the slight remaining difference is assessed by exchanging the Dalitz template for one of the charged hadrons measured in data and scaling the resulting difference by an estimate of the contamination [22] relative to the fraction of electrons from Dalitz decays. This results in an uncertainty of 0.009 on the final v_2 in the first p_T interval, falling quickly with p_T . The small ($\ll 1\%$) contributions from the decay of strange particles are accounted for by the Dalitz and conversion electron templates. Because of the long lifetime, this contribution has a wide impact parameter distribution. The unaccounted contribution of these strange decay electrons is negligible within the applied d_0 range of $[-0.1, 0.1]$ cm in the fitting procedure [52].

The template fits are based on the method proposed in Ref. [58] and implemented as in Ref. [52]. Figure 1 shows examples of the resulting fits in in plane (left panel) and out of plane (right panel) of electron d_0 distributions for the interval $2.5 < p_T < 3$ GeV/c. In the figure the MC templates are corrected for all effects described in the following.

Detailed corrections to the MC templates are applied in order to take into account effects not simulated in MC simulations. Special care is taken to assess differences in the in-plane and out-of-plane templates as the effects of the corrections do not cancel in the computation of the v_2 . The main corrections applied in the MC simulations are (i) resolution of the d_0 distribution, (ii) misassociated electrons from photon conversions and their multiplicity dependence, (iii) p_T distribution of charm and beauty

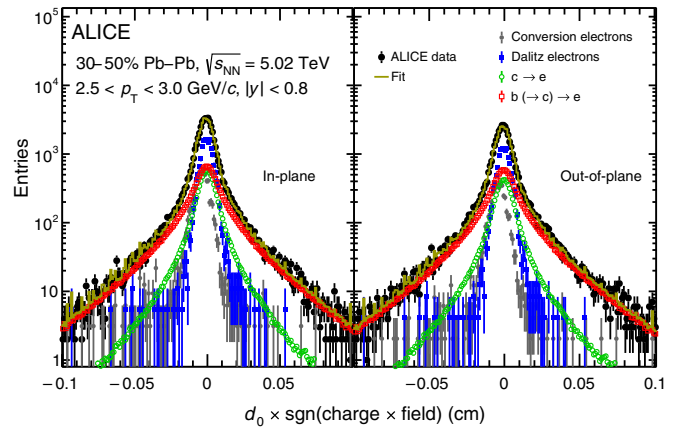


FIG. 1. Examples of the electron transverse impact parameter fits in plane (left) and out of plane (right) for $2.5 < p_T < 3$ GeV/c. Distributions from data and the four MC templates, electrons from beauty ($b \rightarrow c \rightarrow e$) and charm ($c \rightarrow e$) hadron decays, electrons from photon conversions (conversion electrons) and from other sources (Dalitz electrons) used in the fit are shown.

hadrons in in plane and out of plane, and (iv) baryon-to-meson ratio of charm and beauty hadrons. A detailed description of these corrections are described below.

To ensure angular isotropy of the d_0 reconstruction in data, the mean d_0 of primary particles is compared in different regions in azimuth, z position, and p_T with a granularity smaller than the detector components and recentered prior to fitting. Depending on p_T , the d_0 resolution in the MC simulations is about 11%–13% better than in data [59,60], so this amount of smearing is added to make the MC simulations and data match. Primary pions and kaons are used for the comparison. It is observed that the resolution of the impact parameter does not depend significantly on the local track density.

The correct template shape of electrons from photon conversions depends on the production vertex and on the track multiplicity. In-plane and out-of-plane events have different local track densities, requiring separate corrections for the respective templates. This is achieved by choosing different centrality ranges for each template in the simulations. The ranges are defined based on how well they describe either the in-plane or out-of-plane reconstruction efficiencies of pions from K_S^0 decays, as the production vertex of these decays is more accurately reconstructed. The systematic uncertainties are estimated by varying the nominal centrality classes in the simulations and are estimated to be 0.006 at low p_T and decreases to 0.001 with increasing p_T .

Because electrons of a given momentum from heavy-flavor hadron decays may originate from parent particles that have a broader momentum range, their d_0 distributions depend on the p_T distributions of these parent particles. Hence it is necessary to correct for any difference in the p_T distribution of particles that decay to electrons between

data and MC simulations. For the charm case, this can be done by making use of the measured charm mesons p_T spectral shape and v_2 at the same collision energy [26,61]. From these measurements, separate p_T distributions and thus corrections are used for the in-plane and out-of-plane templates. To conservatively assess the uncertainty in the extracted v_2 , the result is compared to a case where the assumed D meson v_2 is halved. An absolute systematic uncertainty of 0.004 is assigned from this comparison to the v_2 of electron from beauty hadron decay.

As there is no available measurement of the low- p_T beauty hadron v_2 , the corrections for the beauty template are determined by using FONLL calculations [62] multiplied by p_T -dependent corrections that are estimated using a range of R_{AA} and v_2 values. The upper limit of the estimated R_{AA} value is the case of no suppression, $R_{AA} = 1$, while the lower limit is obtained by interpolating the TAMU prediction [38], which is consistent with measurements of $R_{AA} \approx 0.4$ at high p_T [52]. The arithmetic mean of the resulting v_2 values is used for the central points of the measurement, with the two limits used to estimate the systematic uncertainty. An absolute systematic variation of 0.0023 at low p_T and of 0.011 at high p_T is found and assigned as an uncertainty. A significant effect arises from the modification of the p_T spectra due to beauty-hadron v_2 since it gives a different correction for the in-plane and out-of-plane templates. For the central value of the measurement, the assumption of $v_2 = 0.014 \times p_T^2 e^{(-1/3 \times p_T)}$ (with p_T in units of GeV/c) is chosen as a generic function inspired by the prediction of the TAMU model [38]. The systematic uncertainty is conservatively evaluated by varying the v_2 value from zero to two times as large, the latter giving a peak of 0.14. For these variations, the change in the measured beauty hadron decay electron v_2 is much smaller than the variation of the assumed hadron v_2 . This gives a flat systematic uncertainty of 0.006 up to $p_T = 4$ GeV/c and of 0.012 in the last p_T interval.

The impact parameter distribution of electrons from the different charm and beauty hadrons depends on the lifetime of these parent hadrons. Therefore, uncertainty in the relative contributions from different parents will translate into uncertainty in the d_0 distribution. For charm, the largest lifetime difference is in the decays of the baryons with respect to the mesons, while for beauty the lifetime of mesons and baryons are very similar and the effect of their different fractions in MC simulation compared to data is negligible. For the charm case, a p_T -dependent correction is applied to the Λ_c/D^0 fraction based on model predictions [63–65], which describe experimental measurements [66–68]. This is compared to a p_T -independent correction that increases the Λ_c/D^0 by a factor of 3. The comparison shows no difference in v_2 for the two scenarios due to the effects canceling out in the computation of the v_2 .

The multiplicity dependence of the efficiency of the particle identification from the TOF detector is evaluated as

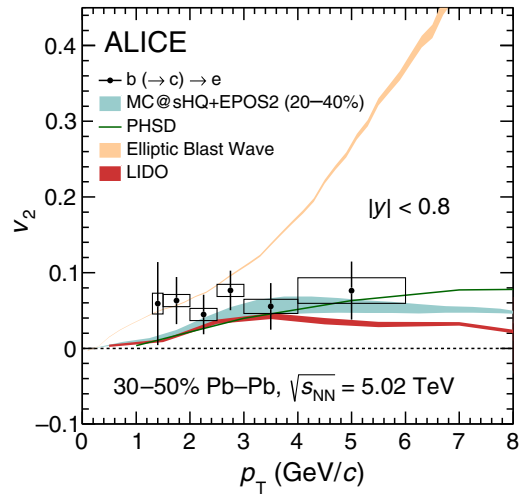


FIG. 2. Elliptic flow of electrons from beauty hadron decays in the 30%–50% centrality class in Pb-Pb collisions at $\sqrt{s_{NN}} = 5.02$ TeV at midrapidity as a function of p_T compared with model calculations [30–32,69].

in Ref. [52]. The efficiencies in plane and out of plane are found to be within 0.5% of each other, which results in an uncertainty of 0.0014 on the v_2 . No multiplicity dependence is found for the efficiency of particle identification from the TPC.

Figure 2 shows the measured v_2 of electrons from beauty hadron decays at midrapidity ($|y| < 0.8$) as a function of p_T in Pb-Pb collisions at $\sqrt{s_{NN}} = 5.02$ TeV in the 30%–50% centrality interval. A positive v_2 of electrons from beauty hadron decays with a significance of 3.75σ is observed for the first time in this low p_T range (1.3–6 GeV/c) using the average v_2 divided by the uncertainty as a test statistic. The systematic uncertainties are assumed to be fully correlated for this purpose. No significant p_T dependence of the v_2 is observed.

The measured v_2 of beauty decay electrons is compared to the predictions from several transport models which include significant interaction of beauty quarks with a hydrodynamically expanding QGP [30–32,69]. These models are observed to well describe the D meson anisotropy and suppression in heavy-ion collisions at the LHC [23–27,70–72]. The MC@sHQ + EPOS [30] is a perturbative QCD model which includes radiative and collisional energy losses. The uncertainties of the model calculations are evaluated by varying from pure collisional to pure radiative energy losses, including also different scattering rates and different rescaling factors. Modification of nuclear parton distribution functions, due to effects from shadowing, for example, is not considered for b quarks. The LIDO model [32,69] also includes both radiative and collisional energy loss. This model uses experimental data to calibrate a Langevin-based transport model and extracts the transport coefficients directly from data via a Bayesian analysis. In the case of LIDO, the reported model

uncertainties are purely statistical. Within this model, the v_2 for beauty hadrons is much smaller than for charm hadrons. The PHSD model [31] is a microscopic off-shell transport model based on a Boltzmann approach which includes only collisional energy loss. Initial-state event-by-event fluctuations are included in all transport models described here. Even though the models differ in several aspects related to the interactions both in the QGP and in the hadronic phase as well as to the medium expansion, they all provide a fair description of the measurement. Similar agreement among these models was previously observed when compared to the R_{AA} of electrons from beauty-hadron decays [52]. With the current experimental uncertainties, no model is clearly favored or disfavored. A model calculation based on an extension of the blast-wave model [47] is also compared with the measurement. The calculation shown is based on B^0 mesons, and the PYTHIA8 decayer is used for their decays into electrons [73]. Assuming full thermalization, this model predicts a v_2 of $\Upsilon(1S)$ close to zero in the range measured by ALICE, which is consistent with the measurement. The results for beauty hadron decay electrons give a much larger v_2 than that of $\Upsilon(1S)$ due to the mass ordering effect. This shows that the measurement presented here is suitable to assess the degree of thermalization of beauty quarks at low p_T . The error band represents purely the statistical uncertainty. This simple model is qualitatively in agreement with the measurement within the uncertainties for $p_T < 3$ GeV/ c , while it significantly diverges from the data at higher p_T .

In summary, the measurement of the elliptic flow of electrons originating from beauty hadron decays at mid-rapidity in semicentral Pb-Pb collisions at $\sqrt{s_{NN}} = 5.02$ TeV is presented for the first time in this low p_T interval 1.3–6 GeV/ c . The measurement is important for the understanding of the degree of thermalization of beauty quarks in the QGP. The v_2 of electrons from beauty hadron decays is found to be positive with a significance of 3.75σ . The measurement provides new insights and constraints to theoretical models of beauty quark interactions in the QGP.

The ALICE Collaboration would like to thank all its engineers and technicians for their invaluable contributions to the construction of the experiment and the CERN accelerator teams for the outstanding performance of the LHC complex. The ALICE Collaboration gratefully acknowledges the resources and support provided by all Grid centres and the Worldwide LHC Computing Grid (WLCG) Collaboration. The ALICE Collaboration acknowledges the following funding agencies for their support in building and running the ALICE detector: A. I. Alikhanyan National Science Laboratory (Yerevan Physics Institute) Foundation (ANSL), State Committee of Science and World Federation of Scientists (WFS), Armenia; Austrian Academy of Sciences, Austrian Science Fund (FWF): [M 2467-N36] and Nationalstiftung für Forschung, Technologie und Entwicklung, Austria; Ministry of

Communications and High Technologies, National Nuclear Research Center, Azerbaijan; Conselho Nacional de Desenvolvimento Científico e Tecnológico (CNPq), Financiadora de Estudos e Projetos (Finep), Fundação de Amparo à Pesquisa do Estado de São Paulo (FAPESP) and Universidade Federal do Rio Grande do Sul (UFRGS), Brazil; Ministry of Education of China (MOEC), Ministry of Science & Technology of China (MSTC) and National Natural Science Foundation of China (NSFC), China; Ministry of Science and Education and Croatian Science Foundation, Croatia; Centro de Aplicaciones Tecnológicas y Desarrollo Nuclear (CEADEN), Cubaenergía, Cuba; Ministry of Education, Youth and Sports of the Czech Republic, Czech Republic; The Danish Council for Independent Research | Natural Sciences, the VILLUM FONDEN and Danish National Research Foundation (DNRF), Denmark; Helsinki Institute of Physics (HIP), Finland; Commissariat à l’Energie Atomique (CEA) and Institut National de Physique Nucléaire et de Physique des Particules (IN2P3) and Centre National de la Recherche Scientifique (CNRS), France; Bundesministerium für Bildung und Forschung (BMBF) and GSI Helmholtzzentrum für Schwerionenforschung GmbH, Germany; General Secretariat for Research and Technology, Ministry of Education, Research and Religions, Greece; National Research, Development and Innovation Office, Hungary; Department of Atomic Energy Government of India (DAE), Department of Science and Technology, Government of India (DST), University Grants Commission, Government of India (UGC) and Council of Scientific and Industrial Research (CSIR), India; Indonesian Institute of Science, Indonesia; Centro Fermi-Museo Storico della Fisica e Centro Studi e Ricerche Enrico Fermi and Istituto Nazionale di Fisica Nucleare (INFN), Italy; Institute for Innovative Science and Technology, Nagasaki Institute of Applied Science (IIST), Japanese Ministry of Education, Culture, Sports, Science and Technology (MEXT) and Japan Society for the Promotion of Science (JSPS) KAKENHI, Japan; Consejo Nacional de Ciencia (CONACYT) y Tecnología, through Fondo de Cooperación Internacional en Ciencia y Tecnología (FONCICYT) and Dirección General de Asuntos del Personal Académico (DGAPA), Mexico; Nederlandse Organisatie voor Wetenschappelijk Onderzoek (NWO), Netherlands; The Research Council of Norway, Norway; Commission on Science and Technology for Sustainable Development in the South (COMSATS), Pakistan; Pontificia Universidad Católica del Perú, Peru; Ministry of Science and Higher Education, National Science Centre and WUT ID-UB, Poland; Korea Institute of Science and Technology Information and National Research Foundation of Korea (NRF), Republic of Korea; Ministry of Education and Scientific Research, Institute of Atomic Physics and Ministry of Research and Innovation and Institute of

Atomic Physics, Romania; Joint Institute for Nuclear Research (JINR), Ministry of Education and Science of the Russian Federation, National Research Centre Kurchatov Institute, Russian Science Foundation and Russian Foundation for Basic Research, Russia; Ministry of Education, Science, Research and Sport of the Slovak Republic, Slovakia; National Research Foundation of South Africa, South Africa; Swedish Research Council (VR) and Knut & Alice Wallenberg Foundation (KAW), Sweden; European Organization for Nuclear Research, Switzerland; Suranaree University of Technology (SUT), National Science and Technology Development Agency (NSDTA) and Office of the Higher Education Commission under NRU project of Thailand, Thailand; Turkish Atomic Energy Agency (TAEK), Turkey; National Academy of Sciences of Ukraine, Ukraine; Science and Technology Facilities Council (STFC), United Kingdom; National Science Foundation of the United States of America (NSF) and United States Department of Energy, Office of Nuclear Physics (DOE NP), United States of America.

-
- [1] K. Aamodt *et al.* (ALICE Collaboration), The ALICE experiment at the CERN LHC, *J. Instrum.* **3**, S08002 (2008).
- [2] F. Karsch, Lattice simulations of the thermodynamics of strongly interacting elementary particles and the exploration of new phases of matter in relativistic heavy ion collisions, *J. Phys. Conf. Ser.* **46**, 122 (2006).
- [3] S. Borsanyi, Z. Fodor, C. Hoelbling, S. D. Katz, S. Krieg, C. Ratti, and K. K. Szabo (Wuppertal-Budapest Collaboration), Is there still any T_c mystery in lattice QCD? Results with physical masses in the continuum limit III, *J. High Energy Phys.* **09** (2010) 073.
- [4] S. Borsanyi, G. Endrodi, Z. Fodor, A. Jakovac, S. D. Katz, S. Krieg, C. Ratti, and K. K. Szabo (Wuppertal-Budapest Collaboration), The QCD equation of state with dynamical quarks, *J. High Energy Phys.* **11** (2010) 077.
- [5] A. Bazavov, T. Bhattacharya, M. Cheng, C. DeTar, H. T. Ding *et al.*, The chiral and deconfinement aspects of the QCD transition, *Phys. Rev. D* **85**, 054503 (2012).
- [6] P. Petreczky, Review of recent highlights in lattice calculations at finite temperature and finite density, *Proc. Sci. ConfinementX2012* (2012) 028 [arXiv:1301.6188].
- [7] M. Gyulassy and M. Plumer, Jet quenching in dense matter, *Phys. Lett. B* **243**, 432 (1990).
- [8] R. Baier, Y. L. Dokshitzer, A. H. Mueller, S. Peigne, and D. Schiff, Radiative energy loss and p_T -broadening of high-energy partons in nuclei, *Nucl. Phys.* **B484**, 265 (1997).
- [9] M. H. Thoma and M. Gyulassy, Quark damping and energy loss in the high temperature QCD, *Nucl. Phys.* **B351**, 491 (1991).
- [10] E. Braaten and M. H. Thoma, Energy loss of a heavy fermion in a hot QED plasma, *Phys. Rev. D* **44**, 1298 (1991).
- [11] E. Braaten and M. H. Thoma, Energy loss of a heavy quark in the quark-gluon plasma, *Phys. Rev. D* **44**, R2625 (1991).
- [12] R. Snellings, Elliptic flow: A brief review, *New J. Phys.* **13**, 055008 (2011).
- [13] S. Voloshin and Y. Zhang, Flow study in relativistic nuclear collisions by Fourier expansion of Azimuthal particle distributions, *Z. Phys. C* **70**, 665 (1996).
- [14] U. Heinz and R. Snellings, Collective flow and viscosity in relativistic heavy-ion collisions, *Annu. Rev. Nucl. Part. Sci.* **63**, 123 (2013).
- [15] H. Niemi, K. J. Eskola, and R. Paatelainen, Event-by-event fluctuations in a perturbative QCD + saturation+hydrodynamics model: Determining QCD matter shear viscosity in ultrarelativistic heavy-ion collisions, *Phys. Rev. C* **93**, 024907 (2016).
- [16] J. E. Bernhard, J. S. Moreland, S. A. Bass, J. Liu, and U. Heinz, Applying Bayesian parameter estimation to relativistic heavy-ion collisions: Simultaneous characterization of the initial state and quark-gluon plasma medium, *Phys. Rev. C* **94**, 024907 (2016).
- [17] A. Dubla, S. Masiocchi, J. M. Pawłowski, B. Schenke, C. Shen, and J. Stachel, Towards QCD-assisted hydrodynamics for heavy-ion collision phenomenology, *Nucl. Phys.* **A979**, 251 (2018).
- [18] M. Gyulassy, I. Vitev, and X. N. Wang, High p_T Azimuthal Asymmetry in Non-Central A + A at RHIC, *Phys. Rev. Lett.* **86**, 2537 (2001).
- [19] E. V. Shuryak, Azimuthal asymmetry at large p_T seem to be too large for a pure jet quenching, *Phys. Rev. C* **66**, 027902 (2002).
- [20] J. Noronha-Hostler, B. Betz, J. Noronha, and M. Gyulassy, Event-by-Event Hydrodynamics + Jet Energy Loss: A Solution to the $R_{AA} \otimes v_2$ Puzzle, *Phys. Rev. Lett.* **116**, 252301 (2016).
- [21] L. Adamczyk *et al.* (STAR Collaboration), Measurement of D^0 Azimuthal Anisotropy at Midrapidity in Au + Au Collisions at $\sqrt{s_{NN}} = 200$ GeV, *Phys. Rev. Lett.* **118**, 212301 (2017).
- [22] S. Acharya *et al.* (ALICE Collaboration), Measurement of electrons from semileptonic heavy-flavour hadron decays at midrapidity in pp and Pb-Pb collisions at $\sqrt{s_{NN}} = 5.02$ TeV, *Phys. Lett. B* **804**, 135377 (2020).
- [23] B. Abelev *et al.* (ALICE Collaboration), D Meson Elliptic Flow in Non-Central Pb-Pb Collisions at Energy $\sqrt{s_{NN}} = 2.76$ TeV, *Phys. Rev. Lett.* **111**, 102301 (2013).
- [24] S. Acharya *et al.* (ALICE Collaboration), Event-shape engineering for the D-meson elliptic flow in mid-central Pb-Pb collisions at $\sqrt{s_{NN}} = 5.02$ TeV, *J. High Energy Phys.* **02** (2019) 150.
- [25] B. Abelev *et al.* (ALICE Collaboration), Azimuthal anisotropy of D meson production in Pb-Pb collisions at energy $\sqrt{s_{NN}} = 2.76$ TeV, *Phys. Rev. C* **90**, 034904 (2014).
- [26] S. Acharya *et al.* (ALICE Collaboration), D-Meson Azimuthal Anisotropy in Midcentral Pb-Pb Collisions at $\sqrt{s_{NN}} = 5.02$ TeV, *Phys. Rev. Lett.* **120**, 102301 (2018).
- [27] A. M. Sirunyan *et al.* (CMS Collaboration), Measurement of Prompt D^0 Meson Azimuthal Anisotropy in Pb-Pb Collisions at $\sqrt{s_{NN}} = 5.02$ TeV, *Phys. Rev. Lett.* **120**, 202301 (2018).

- [28] S. Acharya *et al.* (ALICE Collaboration), J/ψ Elliptic Flow in Pb-Pb Collisions at $\sqrt{s_{NN}} = 5.02$ TeV, *Phys. Rev. Lett.* **119**, 242301 (2017).
- [29] A. Beraudo, A. De Pace, M. Monteno, M. Nardi, and F. Prino, Development of heavy-flavour flow-harmonics in high-energy nuclear collisions, *J. High Energy Phys.* **02** (2018) 043.
- [30] M. Nahrgang, J. Aichelin, P. B. Gossiaux, and K. Werner, Influence of hadronic bound states above T_c on heavy-quark observables in Pb–Pb collisions at the CERN large hadron collider, *Phys. Rev. C* **89**, 014905 (2014).
- [31] T. Song, H. Berrehrah, D. Cabrera, W. Cassing, and E. Bratkovskaya, Charm production in Pb + Pb collisions at energies available at the CERN large hadron collider, *Phys. Rev. C* **93**, 034906 (2016).
- [32] W. Ke, Y. Xu, and S. A. Bass, Modified Boltzmann approach for modeling the splitting vertices induced by the hot QCD medium in the deep Landau-Pomeranchuk-Migdal region, *Phys. Rev. C* **100**, 064911 (2019).
- [33] R. Katz, C. A. G. Prado, J. Noronha-Hostler, J. Noronha, and A. A. P. Suaide, DAB-MOD sensitivity study of heavy flavor R_{AA} and azimuthal anisotropies based on beam energy, initial conditions, hadronization, and suppression mechanisms, *Phys. Rev. C* **102**, 024906 (2020).
- [34] M. He, R. J. Fries, and R. Rapp, Heavy-quark diffusion and hadronization in quark-gluon plasma, *Phys. Rev. C* **86**, 014903 (2012).
- [35] D. Zigic, I. Salom, J. Auvinen, M. Djordjevic, and M. Djordjevic, DREENA-B framework: First predictions of R_{AA} and v_2 within dynamical energy loss formalism in evolving QCD medium, *Phys. Lett. B* **791**, 236 (2019).
- [36] V. Greco, C. M. Ko, and R. Rapp, Quark coalescence for charmed mesons in ultrarelativistic heavy ion collisions, *Phys. Lett. B* **595**, 202 (2004).
- [37] S. Batsouli, S. Kelly, M. Gyulassy, and J. L. Nagle, Does the charm flow at RHIC?, *Phys. Lett. B* **557**, 26 (2003).
- [38] M. He, R. J. Fries, and R. Rapp, Heavy flavor at the large hadron collider in a strong coupling approach, *Phys. Lett. B* **735**, 445 (2014).
- [39] L. Adamczyk *et al.* (STAR Collaboration), Elliptic flow of electrons from heavy-flavor hadron decays in Au + Au collisions at $\sqrt{s_{NN}} = 200$, 62.4, and 39 GeV, *Phys. Rev. C* **95**, 034907 (2017).
- [40] A. Adare *et al.* (PHENIX Collaboration), Energy Loss and Flow of Heavy Quarks in Au + Au Collisions at $\sqrt{s_{NN}} = 200$ GeV, *Phys. Rev. Lett.* **98**, 172301 (2007).
- [41] J. Adam *et al.* (ALICE Collaboration), Elliptic flow of electrons from heavy-flavour hadron decays at mid-rapidity in Pb-Pb collisions at $\sqrt{s_{NN}} = 2.76$ TeV, *J. High Energy Phys.* **09** (2016) 028.
- [42] M. Aaboud *et al.* (ATLAS Collaboration), Measurement of the suppression and azimuthal anisotropy of muons from heavy-flavor decays in Pb + Pb collisions at $\sqrt{s_{NN}} = 2.76$ TeV with the ATLAS detector, *Phys. Rev. C* **98**, 044905 (2018).
- [43] V. Khachatryan *et al.* (CMS Collaboration), Suppression and azimuthal anisotropy of prompt and nonprompt J/ψ production in PbPb collisions at $\sqrt{s_{NN}} = 2.76$ TeV, *Eur. Phys. J. C* **77**, 252 (2017).
- [44] S. Acharya *et al.* (ALICE Collaboration), Measurement of $\Upsilon(1S)$ Elliptic Flow at Forward Rapidity in Pb-Pb Collisions at $\sqrt{s_{NN}} = 5.02$ TeV, *Phys. Rev. Lett.* **123**, 192301 (2019).
- [45] X. Du, R. Rapp, and M. He, Color screening and regeneration of bottomonia in high-energy heavy-ion collisions, *Phys. Rev. C* **96**, 054901 (2017).
- [46] P. P. Bhaduri, N. Borghini, A. Jaiswal, and M. Strickland, Anisotropic escape mechanism and elliptic flow of bottomonia, *Phys. Rev. C* **100**, 051901 (2019).
- [47] K. Reygers, A. Schmah, A. Berdnikova, and X. Sun, Blast-wave description of Upsilon elliptic flow at LHC energies, *Phys. Rev. C* **101**, 064905 (2020).
- [48] G. Aad *et al.* (ATLAS Collaboration), Measurement of azimuthal anisotropy of muons from charm and bottom hadrons in Pb + Pb collisions at $\sqrt{s_{NN}} = 5.02$ TeV with the ATLAS detector, *Phys. Lett. B* **807**, 135595 (2020).
- [49] B. Abelev *et al.* (ALICE Collaboration), Performance of the ALICE experiment at the CERN LHC, *Int. J. Mod. Phys. A* **29**, 1430044 (2014).
- [50] E. Abbas *et al.* (ALICE Collaboration), Performance of the ALICE VZERO system, *J. Instrum.* **8**, P10016 (2013).
- [51] B. Abelev *et al.* (ALICE Collaboration), Centrality determination of Pb-Pb collisions at $\sqrt{s_{NN}} = 2.76$ TeV with ALICE, *Phys. Rev. C* **88**, 044909 (2013).
- [52] J. Adam *et al.* (ALICE Collaboration), Measurement of electrons from beauty-hadron decays in p-Pb collisions at $\sqrt{s_{NN}} = 5.02$ TeV and Pb-Pb collisions at $\sqrt{s_{NN}} = 2.76$ TeV, *J. High Energy Phys.* **07** (2017) 052.
- [53] S. Acharya *et al.* (ALICE Collaboration), Anisotropic flow of identified particles in Pb-Pb collisions at $\sqrt{s_{NN}} = 5.02$ TeV, *J. High Energy Phys.* **09** (2018) 006.
- [54] I. Selyuzhenkov and S. Voloshin, Effects of non-uniform acceptance in anisotropic flow measurement, *Phys. Rev. C* **77**, 034904 (2008).
- [55] M. Gyulassy and X.-N. Wang, HIJING 1.0: A Monte Carlo program for parton and particle production in high-energy hadronic and nuclear collisions, *Comput. Phys. Commun.* **83**, 307 (1994).
- [56] T. Sjostrand, S. Mrenna, and P. Z. Skands, PYTHIA 6.4 physics and manual, *J. High Energy Phys.* **05** (2006) 026.
- [57] R. Brun, F. Bruyant, F. Carminati, S. Giani, M. Maire, A. McPherson, G. Patrick, and L. Urban, *GEANT: Detector Description and Simulation Tool; Oct 1994*, CERN Program Library (CERN, Geneva, 1993), <https://cds.cern.ch/record/1082634>. Long Writeup W5013.
- [58] R. Barlow and C. Beeston, Fitting using finite monte carlo samples, *Comput. Phys. Commun.* **77**, 219 (1993).
- [59] B. Abelev *et al.* (ALICE Collaboration), Performance of the ALICE experiment at the CERN LHC, *Int. J. Mod. Phys. A* **29**, 1430044 (2014).
- [60] B. Abelev *et al.* (ALICE Collaboration), Suppression of high transverse momentum D mesons in central Pb-Pb collisions at $\sqrt{s_{NN}} = 2.76$ TeV, *J. High Energy Phys.* **09** (2012) 112.
- [61] S. Acharya *et al.* (ALICE Collaboration), Measurement of D^0 , D^+ , D^{*+} and D_s^+ production in Pb-Pb collisions at $\sqrt{s_{NN}} = 5.02$ TeV, *J. High Energy Phys.* **10** (2018) 174.

- [62] M. Cacciari, M. Greco, and P. Nason, The p_T spectrum in heavy flavor hadroproduction, *J. High Energy Phys.* **05** (1998) 007.
- [63] A. Andronic, P. Braun-Munzinger, M. K. Köhler, K. Redlich, and J. Stachel, Transverse momentum distributions of charmonium states with the statistical hadronization model, *Phys. Lett. B* **797**, 134836 (2019).
- [64] S. Plumari, V. Minissale, S. K. Das, G. Coci, and V. Greco, Charmed hadrons from coalescence plus fragmentation in relativistic nucleus-nucleus collisions at RHIC and LHC, *Eur. Phys. J. C* **78**, 348 (2018).
- [65] J. Song, H.-h. Li, and F.-l. Shao, New feature of low p_T charm quark hadronization in pp collisions at $\sqrt{s} = 7$ TeV, *Eur. Phys. J. C* **78**, 344 (2018).
- [66] S. Acharya *et al.* (ALICE Collaboration), Λ_c^+ production in Pb-Pb collisions at $\sqrt{s_{NN}} = 5.02$ TeV, *Phys. Lett. B* **793**, 212 (2019).
- [67] J. Adam *et al.* (STAR Collaboration), Observation of Enhancement of Charmed Baryon-to-Meson Ratio in Au + Au Collisions at $\sqrt{s_{NN}} = 200$ GeV, *Phys. Rev. Lett.* **124**, 172301 (2020).
- [68] A. M. Sirunyan *et al.* (CMS Collaboration), Production of Λ_c^+ baryons in proton-proton and lead-lead collisions at $\sqrt{s_{NN}} = 5.02$ TeV, *Phys. Lett. B* **803**, 135328 (2020).
- [69] W. Ke, Y. Xu, and S. A. Bass, Linearized Boltzmann-Langevin model for heavy quark transport in hot and dense QCD matter, *Phys. Rev. C* **98**, 064901 (2018).
- [70] B. Abelev *et al.* (ALICE Collaboration), Suppression of high transverse momentum D mesons in central Pb-Pb collisions at energy $\sqrt{s_{NN}} = 2.76$ TeV, *J. High Energy Phys.* **09** (2012) 112.
- [71] J. Adam *et al.* (ALICE Collaboration), Centrality dependence of high- p_T D meson suppression in Pb-Pb collisions at $\sqrt{s_{NN}} = 2.76$ TeV, *J. High Energy Phys.* **11** (2015) 205; **06** (2017) 032(A).
- [72] A. M. Sirunyan *et al.* (CMS Collaboration), Nuclear modification factor of D^0 mesons in PbPb collisions at $\sqrt{s_{NN}} = 5.02$ TeV, *Phys. Lett. B* **782**, 474 (2018).
- [73] T. Sjöstrand, S. Ask, J. R. Christiansen, R. Corke, N. Desai, P. Ilten, S. Mrenna, S. Prestel, C. O. Rasmussen, and P. Z. Skands, An introduction to PYTHIA 8.2, *Comput. Phys. Commun.* **191**, 159 (2015).

S. Acharya,¹⁴¹ D. Adamová,⁹⁵ A. Adler,⁷⁴ J. Adolfsson,⁸¹ M. M. Aggarwal,¹⁰⁰ G. Aglieri Rinella,³⁴ M. Agnello,³⁰ N. Agrawal,^{10,54} Z. Ahammed,¹⁴¹ S. Ahmad,¹⁶ S. U. Ahn,⁷⁶ Z. Akbar,⁵¹ A. Akindinov,⁹² M. Al-Turany,¹⁰⁷ S. N. Alam,^{40,141} D. S. D. Albuquerque,¹²² D. Aleksandrov,⁸⁸ B. Alessandro,⁵⁹ H. M. Alfanda,⁶ R. Alfaro Molina,⁷¹ B. Ali,¹⁶ Y. Ali,¹⁴ A. Alici,^{10,26a,26b,54} N. Alizadehvandchali,¹²⁵ A. Alkin,^{2,34} J. Alme,²¹ T. Alt,⁶⁸ L. Altenkamper,²¹ I. Altsybeev,¹¹³ M. N. Anaam,⁶ C. Andrei,⁴⁸ D. Andreou,³⁴ A. Andronic,¹⁴⁴ M. Angeletti,³⁴ V. Anguelov,¹⁰⁴ C. Anson,¹⁵ T. Antičić,¹⁰⁸ F. Antinori,⁵⁷ P. Antonioli,⁵⁴ N. Apadula,⁸⁰ L. Aphecetche,¹¹⁵ H. Appelshäuser,⁶⁸ S. Arcelli,^{26a,26b} R. Arnaldi,⁵⁹ M. Arratia,⁸⁰ I. C. Arsene,²⁰ M. Arslanodk,¹⁰⁴ A. Augustinus,³⁴ R. Averbeck,¹⁰⁷ S. Aziz,⁷⁸ M. D. Azmi,¹⁶ A. Badalà,⁵⁶ Y. W. Baek,⁴¹ S. Bagnasco,⁵⁹ X. Bai,¹⁰⁷ R. Bailhache,⁶⁸ R. Bala,¹⁰¹ A. Balbino,³⁰ A. Baldisseri,¹³⁷ M. Ball,⁴³ S. Balouza,¹⁰⁵ D. Banerjee,^{3a,3b} R. Barbera,^{27a,27b} L. Barioglio,^{25a,25b} G. G. Barnaföldi,¹⁴⁵ L. S. Barnby,⁹⁴ V. Barret,¹³⁴ P. Bartalini,⁶ C. Bartels,¹²⁷ K. Barth,³⁴ E. Bartsch,⁶⁸ F. Baruffaldi,^{28a,28b} N. Bastid,¹³⁴ S. Basu,¹⁴³ G. Batigne,¹¹⁵ B. Batyunya,⁷⁵ D. Bauri,⁴⁹ J. L. Bazo Alba,¹¹² I. G. Bearden,⁸⁹ C. Beattie,¹⁴⁶ C. Bedda,⁶³ N. K. Behera,⁶¹ I. Belikov,¹³⁶ A. D. C. Bell Hechavarria,¹⁴⁴ F. Bellini,³⁴ R. Bellwied,¹²⁵ V. Belyaev,⁹³ G. Bencedi,¹⁴⁵ S. Beole,^{25a,25b} A. Bercuci,⁴⁸ Y. Berdnikov,⁹⁸ D. Berenyi,¹⁴⁵ R. A. Bertens,¹³⁰ D. Berzano,⁵⁹ M. G. Besoiu,⁶⁷ L. Betev,³⁴ A. Bhasin,¹⁰¹ I. R. Bhat,¹⁰¹ M. A. Bhat,^{3a,3b} H. Bhatt,⁴⁹ B. Bhattacharjee,⁴² A. Bianchi,^{25a,25b} L. Bianchi,^{25a,25b} N. Bianchi,⁵² J. Bielčik,³⁷ J. Bielčíková,⁹⁵ A. Bilandzic,¹⁰⁵ G. Biro,¹⁴⁵ R. Biswas,^{3a,3b} S. Biswas,^{3a,3b} J. T. Blair,¹¹⁹ D. Blau,⁸⁸ C. Blume,⁶⁸ G. Boca,¹³⁹ F. Bock,⁹⁶ A. Bogdanov,⁹³ S. Boi,^{23a,23b} J. Bok,⁶¹ L. Boldizsár,¹⁴⁵ A. Bolozdynya,⁹³ M. Bombara,³⁸ G. Bonomi,¹⁴⁰ H. Borel,¹³⁷ A. Borissov,⁹³ H. Bossi,¹⁴⁶ E. Botta,^{25a,25b} L. Bratrud,⁶⁸ P. Braun-Munzinger,¹⁰⁷ M. Bregant,¹²¹ M. Broz,³⁷ E. Bruna,⁵⁹ G. E. Bruno,^{33a,33b,106} M. D. Buckland,¹²⁷ D. Budnikov,¹⁰⁹ H. Buesching,⁶⁸ S. Bufalino,³⁰ O. Bugnon,¹¹⁵ P. Buhler,¹¹⁴ P. Buncic,³⁴ Z. Buthelezi,^{72,131} J. B. Butt,¹⁴ S. A. Bysiak,¹¹⁸ D. Caffarri,⁹⁰ A. Caliva,¹⁰⁷ E. Calvo Villar,¹¹² J. M. M. Camacho,¹²⁰ R. S. Camacho,⁴⁵ P. Camerini,^{24a,24b} F. D. M. Canedo,¹²¹ A. A. Capon,¹¹⁴ F. Carnesecci,^{26a,26b} R. Caron,¹³⁷ J. Castillo Castellanos,¹³⁷ A. J. Castro,¹³⁰ E. A. R. Casula,⁵⁵ F. Catalano,³⁰ C. Ceballos Sanchez,⁷⁵ P. Chakraborty,⁴⁹ S. Chandra,¹⁴¹ W. Chang,⁶ S. Chapeland,³⁴ M. Chartier,¹²⁷ S. Chattopadhyay,¹⁴¹ S. Chattopadhyay,¹¹⁰ A. Chauvin,^{23a,23b} C. Cheshkov,¹³⁵ B. Cheynis,¹³⁵ V. Chibante Barroso,³⁴ D. D. Chinellato,¹²² S. Cho,⁶¹ P. Chochula,³⁴ T. Chowdhury,¹³⁴ P. Christakoglou,⁹⁰ C. H. Christensen,⁸⁹ P. Christiansen,⁸¹ T. Chujo,¹³³ C. Cicalo,⁵⁵ L. Cifarelli,^{10,26a,26b} L. D. Cilladi,^{25a,25b} F. Cindolo,⁵⁴ M. R. Ciupek,¹⁰⁷ G. Clai,^{54,a} J. Cleymans,¹²⁴ F. Colamaria,⁵³ D. Colella,⁵³ A. Collu,⁸⁰ M. Colocci,^{26a,26b} M. Concas,^{59,b} G. Conesa Balbastre,⁷⁹ Z. Conesa del Valle,⁷⁸ G. Contin,^{24a,24b,60} J. G. Contreras,³⁷ T. M. Cormier,⁹⁶ Y. Corrales Morales,^{25a,25b} P. Cortese,³¹ M. R. Cosentino,¹²³ F. Costa,³⁴ S. Costanza,¹³⁹ P. Crochet,¹³⁴ E. Cuautle,⁶⁹ P. Cui,⁶ L. Cunqueiro,⁹⁶ D. Dabrowski,¹⁴² T. Dahms,¹⁰⁵ A. Dainese,⁵⁷ F. P. A. Damas,^{115,137} M. C. Danisch,¹⁰⁴ A. Danu,⁶⁷ D. Das,¹¹⁰ I. Das,¹¹⁰ P. Das,⁸⁶ P. Das,^{3a,3b} S. Das,^{3a,3b} A. Dash,⁸⁶ S. Dash,⁴⁹ S. De,⁸⁶ A. De Caro,^{29a,29b} G. de Cataldo,⁵³ J. de Cuveland,³⁹

E. Meninno,^{29a,29b,114} A. S. Menon,¹²⁵ M. Meres,¹³ S. Mhlanga,¹²⁴ Y. Mlake,¹³³ L. Micheletti,^{25a,25b} L. C. Migliorin,¹³⁵
D. L. Mihaylov,¹⁰⁵ K. Mikhaylov,^{75,92} A. N. Mishra,⁶⁹ D. Miśkowiec,¹⁰⁷ A. Modak,^{3a,3b} N. Mohammadi,³⁴ A. P. Mohanty,⁶³
B. Mohanty,⁸⁶ M. Mohisin Khan,^{16,d} Z. Moravcova,⁸⁹ C. Mordasini,¹⁰⁵ D. A. Moreira De Godoy,¹⁴⁴ L. A. P. Moreno,⁴⁵
I. Morozov,⁶² A. Morsch,³⁴ T. Mrnjavac,³⁴ V. Muccifora,⁵² E. Mudnic,³⁵ D. Mühlheim,¹⁴⁴ S. Muhuri,¹⁴¹ J. D. Mulligan,⁸⁰
A. Mulliri,^{23a,23b,55} M. G. Munhoz,¹²¹ R. H. Munzer,⁶⁸ H. Murakami,¹³² S. Murray,¹²⁴ L. Musa,³⁴ J. Musinsky,⁶⁴
C. J. Myers,¹²⁵ J. W. Myrcha,¹⁴² B. Naik,⁴⁹ R. Nair,⁸⁵ B. K. Nandi,⁴⁹ R. Nania,^{10,54} E. Nappi,⁵³ M. U. Naru,¹⁴
A. F. Nassirpour,⁸¹ C. Natrass,¹³⁰ R. Nayak,⁴⁹ T. K. Nayak,⁸⁶ S. Nazarenko,¹⁰⁹ A. Neagu,²⁰ R. A. Negrao De Oliveira,⁶⁸
L. Nellen,⁶⁹ S. V. Nesbo,³⁶ G. Neskovic,³⁹ D. Nesterov,¹¹³ L. T. Neumann,¹⁴² B. S. Nielsen,⁸⁹ S. Nikolaev,⁸⁸ S. Nikulin,⁸⁸
V. Nikulin,⁹⁸ F. Noferini,^{10,54} P. Nomokonov,⁷⁵ J. Norman,^{79,127} N. Novitzky,¹³³ P. Nowakowski,¹⁴² A. Nyanin,⁸⁸
J. Nystrand,²¹ M. Ogino,⁸² A. Ohlson,^{81,104} J. Oleniacz,¹⁴² A. C. Oliveira Da Silva,¹³⁰ M. H. Oliver,¹⁴⁶ C. Oppedisano,⁵⁹
A. Ortiz Velasquez,⁶⁹ A. Oskarsson,⁸¹ J. Otwinowski,¹¹⁸ K. Oyama,⁸² Y. Pachmayer,¹⁰⁴ V. Pacik,⁸⁹ S. Padhan,⁴⁹
D. Pagano,¹⁴⁰ G. Paić,⁶⁹ J. Pan,¹⁴³ S. Panebianco,¹³⁷ P. Pareek,^{50,141} J. Park,⁶¹ J. E. Parkkila,¹²⁶ S. Parmar,¹⁰⁰ S. P. Pathak,¹²⁵
B. Paul,^{23a,23b} J. Pazzini,¹⁴⁰ H. Pei,⁶ T. Peitzmann,⁶³ X. Peng,⁶ L. G. Pereira,⁷⁰ H. Pereira Da Costa,¹³⁷ D. Peresunko,⁸⁸
G. M. Perez,⁸ S. Perrin,¹³⁷ Y. Pestov,⁴ V. Petráček,³⁷ M. Petrovici,⁴⁸ R. P. Pezzi,⁷⁰ S. Piano,⁶⁰ M. Pikna,¹³ P. Pillot,¹¹⁵
O. Pinazza,^{34,54} L. Pinsky,¹²⁵ C. Pinto,^{27a,27b} S. Pisano,^{10,52} D. Pistone,⁵⁶ M. Płoskoń,⁸⁰ M. Planinic,⁹⁹ F. Pliquett,⁶⁸
M. G. Poghosyan,⁹⁶ B. Polichtchouk,⁹¹ N. Poljak,⁹⁹ A. Pop,⁴⁸ S. Porteboeuf-Houssais,¹³⁴ V. Pozdniakov,⁷⁵ S. K. Prasad,^{3a,3b}
R. Preghenella,⁵⁴ F. Prino,⁵⁹ C. A. Pruneau,¹⁴³ I. Pshenichnov,⁶² M. Puccio,³⁴ J. Putschke,¹⁴³ S. Qiu,⁹⁰ L. Quaglia,^{25a,25b}
R. E. Quishpe,¹²⁵ S. Ragoni,¹¹¹ S. Raha,^{3a,3b} S. Rajput,¹⁰¹ J. Rak,¹²⁶ A. Rakotozafindrabe,¹³⁷ L. Ramello,³¹ F. Rami,¹³⁶
S. A. R. Ramirez,⁴⁵ R. Raniwala,¹⁰² S. Raniwala,¹⁰² S. S. Räsänen,⁴⁴ R. Rath,⁵⁰ V. Ratzka,⁴³ I. Ravasenga,⁹⁰ K. F. Read,^{96,130}
A. R. Redelbach,³⁹ K. Redlich,^{85,e} A. Rehman,²¹ P. Reichelt,⁶⁸ F. Reidt,³⁴ X. Ren,⁶ R. Renfordt,⁶⁸ Z. Rescakova,³⁸
K. Reygers,¹⁰⁴ A. Riabov,⁹⁸ V. Riabov,⁹⁸ T. Richert,^{81,89} M. Richter,²⁰ P. Riedler,³⁴ W. Riegler,³⁴ F. Riggi,^{27a,27b} C. Ristea,⁶⁷
S. P. Rode,⁵⁰ M. Rodríguez Cahuantzi,⁴⁵ K. Røed,²⁰ R. Rogalev,⁹¹ E. Rogochaya,⁷⁵ D. Rohr,³⁴ D. Röhrich,²¹ P. F. Rojas,⁴⁵
P. S. Rokita,¹⁴² F. Ronchetti,⁵² A. Rosano,⁵⁶ E. D. Rosas,⁶⁹ K. Roslon,¹⁴² A. Rossi,^{28a,28b,57} A. Rotondi,¹³⁹ A. Roy,⁵⁰
P. Roy,¹¹⁰ O. V. Rueda,⁸¹ R. Rui,^{24a,24b} B. Rumyantsev,⁷⁵ A. Rustamov,⁸⁷ E. Ryabinkin,⁸⁸ Y. Ryabov,⁹⁸ A. Rybicki,¹¹⁸
H. Rytönen,¹²⁶ O. A. M. Saarimaki,⁴⁴ R. Sadek,¹¹⁵ S. Sadhu,¹⁴¹ S. Sadovsky,⁹¹ K. Šafařík,³⁷ S. K. Saha,¹⁴¹ B. Sahoo,⁴⁹
P. Sahoo,⁴⁹ R. Sahoo,⁵⁰ S. Sahoo,⁶⁵ P. K. Sahu,⁶⁵ J. Saini,¹⁴¹ S. Sakai,¹³³ S. Sambyal,¹⁰¹ V. Samsonov,^{93,98} D. Sarkar,¹⁴³
N. Sarkar,¹⁴¹ P. Sarma,⁴² V. M. Sarti,¹⁰⁵ M. H. P. Sas,⁶³ E. Scapparone,⁵⁴ J. Schambach,¹¹⁹ H. S. Scheid,⁶⁸ C. Schiaua,⁴⁸
R. Schicker,¹⁰⁴ A. Schmah,¹⁰⁴ C. Schmidt,¹⁰⁷ H. R. Schmidt,¹⁰³ M. O. Schmidt,¹⁰⁴ M. Schmidt,¹⁰³ N. V. Schmidt,^{68,96}
A. R. Schmier,¹³⁰ J. Schukraft,⁸⁹ Y. Schutz,¹³⁶ K. Schwarz,¹⁰⁷ K. Schweda,¹⁰⁷ G. Scioli,^{26a,26b} E. Scomparin,⁵⁹ J. E. Seger,¹⁵
Y. Sekiguchi,¹³² D. Sekihata,¹³² I. Selyuzhenkov,^{93,107} S. Senyukov,¹³⁶ D. Serebryakov,⁶² A. Sevcenco,⁶⁷ A. Shabanov,⁶²
A. Shabetai,¹¹⁵ R. Shahoyan,³⁴ W. Shaikh,¹¹⁰ A. Shangaraev,⁹¹ A. Sharma,¹⁰⁰ A. Sharma,¹⁰¹ H. Sharma,¹¹⁸ M. Sharma,¹⁰¹
N. Sharma,¹⁰⁰ S. Sharma,¹⁰¹ O. Sheibani,¹²⁵ K. Shigaki,⁴⁶ M. Shimomura,⁸³ S. Shirinkin,⁹² Q. Shou,⁴⁰ Y. Sibiraki,⁸⁸
S. Siddhanta,⁵⁵ T. Siemiarczuk,⁸⁵ D. Silvermyr,⁸¹ G. Simatovic,⁹⁰ G. Simonetti,³⁴ B. Singh,¹⁰⁵ R. Singh,⁸⁶ R. Singh,¹⁰¹
R. Singh,⁵⁰ V. K. Singh,¹⁴¹ V. Singhal,¹⁴¹ T. Sinha,¹¹⁰ B. Sitar,¹³ M. Sitta,³¹ T. B. Skaali,²⁰ M. Slupecki,⁴⁴ N. Smirnov,¹⁴⁶
R. J. M. Snellings,⁶³ C. Soncco,¹¹² J. Song,¹²⁵ A. Songmoolnak,¹¹⁶ F. Soramel,^{28a,28b} S. Sorensen,¹³⁰ I. Sputowska,¹¹⁸
J. Stachel,¹⁰⁴ I. Stan,⁶⁷ P. J. Steffanic,¹³⁰ E. Stenlund,⁸¹ S. F. Stiefelmaier,¹⁰⁴ D. Stocco,¹¹⁵ M. M. Storetvedt,³⁶
L. D. Stritto,^{29a,29b} A. A. P. Suaide,¹²¹ T. Sugitate,⁴⁶ C. Suire,⁷⁸ M. Suleymanov,¹⁴ M. Suljic,³⁴ R. Sultanov,⁹² M. Šumbera,⁹⁵
V. Šumbera,¹⁰¹ S. Sumowidagdo,⁵¹ S. Swain,⁶⁵ A. Szabo,¹³ I. Szarka,¹³ U. Tabassam,¹⁴ S. F. Taghavi,¹⁰⁵ G. Taillepieu,¹³⁴
J. Takahashi,¹²² G. J. Tambave,²¹ S. Tang,^{6,134} M. Tarhini,¹¹⁵ M. G. Tazila,⁴⁸ A. Tauro,³⁴ G. Tejada Muñoz,⁴⁵ A. Telesca,³⁴
L. Terlizzi,^{25a,25b} C. Terrevoli,¹²⁵ D. Thakur,⁵⁰ S. Thakur,¹⁴¹ D. Thomas,¹¹⁹ F. Thoresen,⁸⁹ R. Tieulent,¹³⁵ A. Tikhonov,⁶²
A. R. Timmins,¹²⁵ A. Toia,⁶⁸ N. Topilskaya,⁶² M. Toppi,⁵² F. Torales-Acosta,¹⁹ S. R. Torres,³⁷ A. Trifiró,^{32,56} S. Tripathy,^{50,69}
T. Tripathy,⁴⁹ S. Trogolo,^{28a,28b} G. Trombetta,^{33a,33b} L. Tropp,³⁸ V. Trubnikov,² W. H. Trzaska,¹²⁶ T. P. Trzcinski,¹⁴²
B. A. Trzeciak,^{37,63} A. Tumkin,¹⁰⁹ R. Turrisi,⁵⁷ T. S. Tveter,²⁰ K. Ullaland,²¹ E. N. Umaka,¹²⁵ A. Uras,¹³⁵ G. L. Usai,^{23a,23b}
M. Vala,³⁸ N. Valle,¹³⁹ S. Vallero,⁵⁹ N. van der Kolk,⁶³ L. V. R. van Doremalen,⁶³ M. van Leeuwen,⁶³ P. Vande Vyvre,³⁴
D. Varga,¹⁴⁵ Z. Varga,¹⁴⁵ M. Varga-Kofarago,¹⁴⁵ A. Vargas,⁴⁵ M. Vasileiou,⁸⁴ A. Vasiliev,⁸⁸ O. Vázquez Doce,¹⁰⁵
V. Vechemin,¹¹³ E. Vercellin,^{25a,25b} S. Vergara Limón,⁴⁵ L. Vermunt,⁶³ R. Vernet,⁷ R. Vértesi,¹⁴⁵ L. Vickovic,³⁵
Z. Vilakazi,¹³¹ O. Villalobos Baillie,¹¹¹ G. Vino,⁵³ A. Vinogradov,⁸⁸ T. Virgili,^{29a,29b} V. Vislavicius,⁸⁹ A. Vodopyanov,⁷⁵
B. Volkel,³⁴ M. A. Völkl,¹⁰³ K. Voloshin,⁹² S. A. Voloshin,¹⁴³ G. Volpe,^{33a,33b} B. von Haller,³⁴ I. Vorobyev,¹⁰⁵ D. Voscek,¹¹⁷
J. Vrláková,³⁸ B. Wagner,²¹ M. Weber,¹¹⁴ S. G. Weber,¹⁴⁴ A. Wegrzynek,³⁴ S. C. Wenzel,³⁴ J. P. Wessels,¹⁴⁴ J. Wiechula,⁶⁸

J. Wikne,²⁰ G. Wilk,⁸⁵ J. Wilkinson,^{10,54} G. A. Willems,¹⁴⁴ E. Willsher,¹¹¹ B. Windelband,¹⁰⁴ M. Winn,¹³⁷ W. E. Witt,¹³⁰
 J. R. Wright,¹¹⁹ Y. Wu,¹²⁸ R. Xu,⁶ S. Yalcin,⁷⁷ Y. Yamaguchi,⁴⁶ K. Yamakawa,⁴⁶ S. Yang,²¹ S. Yano,¹³⁷ Z. Yin,⁶
 H. Yokoyama,⁶³ I.-K. Yoo,¹⁷ J. H. Yoon,⁶¹ S. Yuan,²¹ A. Yuncu,¹⁰⁴ V. Yurchenko,² V. Zaccolo,^{24a,24b} A. Zaman,¹⁴
 C. Zampolli,³⁴ H. J. C. Zanoli,⁶³ N. Zardoshti,³⁴ A. Zarochentsev,¹¹³ P. Závada,⁶⁶ N. Zaviyalov,¹⁰⁹ H. Zbroszczyk,¹⁴²
 M. Zhalov,⁹⁸ S. Zhang,⁴⁰ X. Zhang,⁶ Z. Zhang,⁶ V. Zherebchevskii,¹¹³ Y. Zhi,¹² D. Zhou,⁶ Y. Zhou,⁸⁹ Z. Zhou,²¹ J. Zhu,^{6,107}
 Y. Zhu,⁶ A. Zichichi,^{10,26a,26b} G. Zinovjev,² and N. Zurlo¹⁴⁰

(ALICE Collaboration)

¹A.I. Alikhanyan National Science Laboratory (Yerevan Physics Institute) Foundation, Yerevan, Armenia

²Bogolyubov Institute for Theoretical Physics, National Academy of Sciences of Ukraine, Kiev, Ukraine

^{3a}Bose Institute, Department of Physics, Kolkata, India

^{3b}Centre for Astroparticle Physics and Space Science (CAPSS), Kolkata, India

⁴Budker Institute for Nuclear Physics, Novosibirsk, Russia

⁵California Polytechnic State University, San Luis Obispo, California, USA

⁶Central China Normal University, Wuhan, China

⁷Centre de Calcul de l'IN2P3, Villeurbanne, Lyon, France

⁸Centro de Aplicaciones Tecnológicas y Desarrollo Nuclear (CEADEN), Havana, Cuba

⁹Centro de Investigación y de Estudios Avanzados (CINVESTAV), Mexico City and Mérida, Mexico

¹⁰Centro Fermi-Museo Storico della Fisica e Centro Studi e Ricerche "Enrico Fermi," Rome, Italy

¹¹Chicago State University, Chicago, Illinois, USA

¹²China Institute of Atomic Energy, Beijing, China

¹³Comenius University Bratislava, Faculty of Mathematics, Physics and Informatics, Bratislava, Slovakia

¹⁴COMSATS University Islamabad, Islamabad, Pakistan

¹⁵Creighton University, Omaha, Nebraska, USA

¹⁶Department of Physics, Aligarh Muslim University, Aligarh, India

¹⁷Department of Physics, Pusan National University, Pusan, Republic of Korea

¹⁸Department of Physics, Sejong University, Seoul, Republic of Korea

¹⁹Department of Physics, University of California, Berkeley, California, USA

²⁰Department of Physics, University of Oslo, Oslo, Norway

²¹Department of Physics and Technology, University of Bergen, Bergen, Norway

^{22a}Dipartimento di Fisica dell'Università 'La Sapienza', Rome, Italy

^{22b}Sezione INFN, Rome, Italy

^{23a}Dipartimento di Fisica dell'Università, Cagliari, Italy

^{23b}Sezione INFN, Cagliari, Italy

^{24a}Dipartimento di Fisica dell'Università, Trieste, Italy

^{24b}Sezione INFN, Trieste, Italy

^{25a}Dipartimento di Fisica dell'Università, Turin, Italy

^{25b}Sezione INFN, Turin, Italy

^{26a}Dipartimento di Fisica e Astronomia dell'Università, Bologna, Italy

^{26b}Sezione INFN, Bologna, Italy

^{27a}Dipartimento di Fisica e Astronomia dell'Università, Catania, Italy

^{27b}Sezione INFN, Catania, Italy

^{28a}Dipartimento di Fisica e Astronomia dell'Università, Padova, Italy

^{28b}Sezione INFN, Padova, Italy

^{29a}Dipartimento di Fisica 'E.R. Caianiello' dell'Università, Salerno, Italy

^{29b}Gruppo Collegato INFN, Salerno, Italy

³⁰Dipartimento DISAT del Politecnico and Sezione INFN, Turin, Italy

³¹Dipartimento di Scienze e Innovazione Tecnologica dell'Università del Piemonte Orientale and INFN Sezione di Torino,

Alessandria, Italy

³²Dipartimento di Scienze MIFT, Università di Messina, Messina, Italy

^{33a}Dipartimento Interateneo di Fisica 'M. Merlin', Bari, Italy

^{33b}Sezione INFN, Bari, Italy

³⁴European Organization for Nuclear Research (CERN), Geneva, Switzerland

³⁵Faculty of Electrical Engineering, Mechanical Engineering and Naval Architecture, University of Split, Split, Croatia

³⁶Faculty of Engineering and Science, Western Norway University of Applied Sciences, Bergen, Norway

³⁷Faculty of Nuclear Sciences and Physical Engineering, Czech Technical University in Prague, Prague, Czech Republic

- ³⁸Faculty of Science, P.J. Šafárik University, Košice, Slovakia
- ³⁹Frankfurt Institute for Advanced Studies, Johann Wolfgang Goethe-Universität Frankfurt, Frankfurt, Germany
- ⁴⁰Fudan University, Shanghai, China
- ⁴¹Gangneung-Wonju National University, Gangneung, Republic of Korea
- ⁴²Gauhati University, Department of Physics, Guwahati, India
- ⁴³Helmholtz-Institut für Strahlen- und Kernphysik, Rheinische Friedrich-Wilhelms-Universität Bonn, Bonn, Germany
- ⁴⁴Helsinki Institute of Physics (HIP), Helsinki, Finland
- ⁴⁵High Energy Physics Group, Universidad Autónoma de Puebla, Puebla, Mexico
- ⁴⁶Hiroshima University, Hiroshima, Japan
- ⁴⁷Hochschule Worms, Zentrum für Technologietransfer und Telekommunikation (ZTT), Worms, Germany
- ⁴⁸Horia Hulubei National Institute of Physics and Nuclear Engineering, Bucharest, Romania
- ⁴⁹Indian Institute of Technology Bombay (IIT), Mumbai, India
- ⁵⁰Indian Institute of Technology Indore, Indore, India
- ⁵¹Indonesian Institute of Sciences, Jakarta, Indonesia
- ⁵²INFN, Laboratori Nazionali di Frascati, Frascati, Italy
- ⁵³INFN, Sezione di Bari, Bari, Italy
- ⁵⁴INFN, Sezione di Bologna, Bologna, Italy
- ⁵⁵INFN, Sezione di Cagliari, Cagliari, Italy
- ⁵⁶INFN, Sezione di Catania, Catania, Italy
- ⁵⁷INFN, Sezione di Padova, Padova, Italy
- ⁵⁸INFN, Sezione di Roma, Rome, Italy
- ⁵⁹INFN, Sezione di Torino, Turin, Italy
- ⁶⁰INFN, Sezione di Trieste, Trieste, Italy
- ⁶¹Inha University, Incheon, Republic of Korea
- ⁶²Institute for Nuclear Research, Academy of Sciences, Moscow, Russia
- ⁶³Institute for Subatomic Physics, Utrecht University/Nikhef, Utrecht, Netherlands
- ⁶⁴Institute of Experimental Physics, Slovak Academy of Sciences, Košice, Slovakia
- ⁶⁵Institute of Physics, Homi Bhabha National Institute, Bhubaneswar, India
- ⁶⁶Institute of Physics of the Czech Academy of Sciences, Prague, Czech Republic
- ⁶⁷Institute of Space Science (ISS), Bucharest, Romania
- ⁶⁸Institut für Kernphysik, Johann Wolfgang Goethe-Universität Frankfurt, Frankfurt, Germany
- ⁶⁹Instituto de Ciencias Nucleares, Universidad Nacional Autónoma de México, Mexico City, Mexico
- ⁷⁰Instituto de Física, Universidade Federal do Rio Grande do Sul (UFRGS), Porto Alegre, Brazil
- ⁷¹Instituto de Física, Universidad Nacional Autónoma de México, Mexico City, Mexico
- ⁷²iThemba LABS, National Research Foundation, Somerset West, South Africa
- ⁷³Jeonbuk National University, Jeonju, Republic of Korea
- ⁷⁴Johann-Wolfgang-Goethe Universität Frankfurt Institut für Informatik, Fachbereich Informatik und Mathematik, Frankfurt, Germany
- ⁷⁵Joint Institute for Nuclear Research (JINR), Dubna, Russia
- ⁷⁶Korea Institute of Science and Technology Information, Daejeon, Republic of Korea
- ⁷⁷KTO Karatay University, Konya, Turkey
- ⁷⁸Laboratoire de Physique des 2 Infinis, Irène Joliot-Curie, Orsay, France
- ⁷⁹Laboratoire de Physique Subatomique et de Cosmologie, Université Grenoble-Alpes, CNRS-IN2P3, Grenoble, France
- ⁸⁰Lawrence Berkeley National Laboratory, Berkeley, California, USA
- ⁸¹Lund University Department of Physics, Division of Particle Physics, Lund, Sweden
- ⁸²Nagasaki Institute of Applied Science, Nagasaki, Japan
- ⁸³Nara Women's University (NWU), Nara, Japan
- ⁸⁴National and Kapodistrian University of Athens, School of Science, Department of Physics, Athens, Greece
- ⁸⁵National Centre for Nuclear Research, Warsaw, Poland
- ⁸⁶National Institute of Science Education and Research, Homi Bhabha National Institute, Jatni, India
- ⁸⁷National Nuclear Research Center, Baku, Azerbaijan
- ⁸⁸National Research Centre Kurchatov Institute, Moscow, Russia
- ⁸⁹Niels Bohr Institute, University of Copenhagen, Copenhagen, Denmark
- ⁹⁰Nikhef, National institute for subatomic physics, Amsterdam, Netherlands
- ⁹¹NRC Kurchatov Institute IHEP, Protvino, Russia
- ⁹²NRC «Kurchatov» what Institute-ITEP, Moscow, Russia
- ⁹³NRNU Moscow Engineering Physics Institute, Moscow, Russia
- ⁹⁴Nuclear Physics Group, STFC Daresbury Laboratory, Daresbury, United Kingdom
- ⁹⁵Nuclear Physics Institute of the Czech Academy of Sciences, Řež u Prahy, Czech Republic
- ⁹⁶Oak Ridge National Laboratory, Oak Ridge, Tennessee, USA
- ⁹⁷Ohio State University, Columbus, Ohio, USA

- ⁹⁸*Petersburg Nuclear Physics Institute, Gatchina, Russia*
- ⁹⁹*Physics department, Faculty of science, University of Zagreb, Zagreb, Croatia*
- ¹⁰⁰*Physics Department, Panjab University, Chandigarh, India*
- ¹⁰¹*Physics Department, University of Jammu, Jammu, India*
- ¹⁰²*Physics Department, University of Rajasthan, Jaipur, India*
- ¹⁰³*Physikalisches Institut, Eberhard-Karls-Universität Tübingen, Tübingen, Germany*
- ¹⁰⁴*Physikalisches Institut, Ruprecht-Karls-Universität Heidelberg, Heidelberg, Germany*
- ¹⁰⁵*Physik Department, Technische Universität München, Munich, Germany*
- ¹⁰⁶*Politecnico di Bari, Bari, Italy*
- ¹⁰⁷*Research Division and ExtreMe Matter Institute EMMI, GSI Helmholtzzentrum für Schwerionenforschung GmbH, Darmstadt, Germany*
- ¹⁰⁸*Rudjer Bošković Institute, Zagreb, Croatia*
- ¹⁰⁹*Russian Federal Nuclear Center (VNIIEF), Sarov, Russia*
- ¹¹⁰*Saha Institute of Nuclear Physics, Homi Bhabha National Institute, Kolkata, India*
- ¹¹¹*School of Physics and Astronomy, University of Birmingham, Birmingham, United Kingdom*
- ¹¹²*Sección Física, Departamento de Ciencias, Pontificia Universidad Católica del Perú, Lima, Peru*
- ¹¹³*St. Petersburg State University, St. Petersburg, Russia*
- ¹¹⁴*Stefan Meyer Institut für Subatomare Physik (SMI), Vienna, Austria*
- ¹¹⁵*SUBATECH, IMT Atlantique, Université de Nantes, CNRS-IN2P3, Nantes, France*
- ¹¹⁶*Suranaree University of Technology, Nakhon Ratchasima, Thailand*
- ¹¹⁷*Technical University of Košice, Košice, Slovakia*
- ¹¹⁸*The Henryk Niewodniczanski Institute of Nuclear Physics, Polish Academy of Sciences, Cracow, Poland*
- ¹¹⁹*The University of Texas at Austin, Austin, Texas, USA*
- ¹²⁰*Universidad Autónoma de Sinaloa, Culiacán, Mexico*
- ¹²¹*Universidade de São Paulo (USP), São Paulo, Brazil*
- ¹²²*Universidade Estadual de Campinas (UNICAMP), Campinas, Brazil*
- ¹²³*Universidade Federal do ABC, Santo Andre, Brazil*
- ¹²⁴*University of Cape Town, Cape Town, South Africa*
- ¹²⁵*University of Houston, Houston, Texas, USA*
- ¹²⁶*University of Jyväskylä, Jyväskylä, Finland*
- ¹²⁷*University of Liverpool, Liverpool, United Kingdom*
- ¹²⁸*University of Science and Technology of China, Hefei, China*
- ¹²⁹*University of South-Eastern Norway, Tonsberg, Norway*
- ¹³⁰*University of Tennessee, Knoxville, Tennessee, USA*
- ¹³¹*University of the Witwatersrand, Johannesburg, South Africa*
- ¹³²*University of Tokyo, Tokyo, Japan*
- ¹³³*University of Tsukuba, Tsukuba, Japan*
- ¹³⁴*Université Clermont Auvergne, CNRS/IN2P3, LPC, Clermont-Ferrand, France*
- ¹³⁵*Université de Lyon, Université Lyon 1, CNRS/IN2P3, IPN-Lyon, Villeurbanne, Lyon, France*
- ¹³⁶*Université de Strasbourg, CNRS, IPHC UMR 7178, F-67000 Strasbourg, France, Strasbourg, France*
- ¹³⁷*Université Paris-Saclay Centre d'Etudes de Saclay (CEA), IRFU, Département de Physique Nucléaire (DPhN), Saclay, France*
- ¹³⁸*Università degli Studi di Foggia, Foggia, Italy*
- ¹³⁹*Università degli Studi di Pavia, Pavia, Italy*
- ¹⁴⁰*Università di Brescia, Brescia, Italy*
- ¹⁴¹*Variable Energy Cyclotron Centre, Homi Bhabha National Institute, Kolkata, India*
- ¹⁴²*Warsaw University of Technology, Warsaw, Poland*
- ¹⁴³*Wayne State University, Detroit, Michigan, USA*
- ¹⁴⁴*Westfälische Wilhelms-Universität Münster, Institut für Kernphysik, Münster, Germany*
- ¹⁴⁵*Wigner Research Centre for Physics, Budapest, Hungary*
- ¹⁴⁶*Yale University, New Haven, Connecticut, USA*
- ¹⁴⁷*Yonsei University, Seoul, Republic of Korea*

[†]Deceased.

^aAlso at Italian National Agency for New Technologies, Energy and Sustainable Economic Development (ENEA), Bologna, Italy.

^bAlso at Dipartimento DET del Politecnico di Torino, Turin, Italy.

^cAlso at M.V. Lomonosov Moscow State University, D.V. Skobeltsyn Institute of Nuclear, Physics, Moscow, Russia.

^dAlso at Department of Applied Physics, Aligarh Muslim University, Aligarh, India.

^eAlso at Institute of Theoretical Physics, University of Wrocław, Wrocław, Poland.